

Damping by Slow Relaxing Rare Earth Impurities in $\text{Ni}_{80}\text{Fe}_{20}$

G. Woltersdorf,¹ M. Kiessling,¹ G. Meyer,² J.-U. Thiele,² and C. H. Back¹

¹Department of Physics, Universität Regensburg, 93040 Regensburg, Germany

²San Jose Research Center, Hitachi Global Storage Technologies, San Jose, California 95135, USA
(Received 21 February 2008; revised manuscript received 17 February 2009; published 25 June 2009)

Doping $\text{Ni}_{80}\text{Fe}_{20}$ by heavy rare earth atoms alters the magnetic relaxation properties of this material drastically. We show that this effect can be well explained by the slow relaxing impurity mechanism. This process is a consequence of the anisotropy of the on site exchange interaction between the $4f$ magnetic moments and the conduction band. As expected from this model the magnitude of the damping effect scales with the anisotropy of the exchange interaction and increases by an order of magnitude at low temperatures. In addition, our measurements allow us to determine the relaxation time of the $4f$ electrons as a function of temperature.

DOI: 10.1103/PhysRevLett.102.257602

PACS numbers: 76.50.+g, 72.10.Di, 75.50.Bb, 76.90.+d

The dynamic response of magnetic materials is of fundamental interest and is essential for various applications in modern magnetic storage technology. Often it is desirable to tailor the damping parameter and the resonance frequency of magnetic materials independently. While the resonance frequency can be controlled relatively easily by, e.g., controlling the saturation magnetization, it is more difficult to change the Gilbert damping parameter in a controlled way. Recent experiments have demonstrated the ability to modify the damping parameter of transition metals and transition metal alloys by introducing rare earth (RE) impurities [1,2] or $3d$ and $5d$ transition metals [3]. Unfortunately a convincing microscopic understanding of the origin of RE-induced damping in metallic alloys is still missing.

Here, we present experimental results on the magnetization dynamics of thin $\text{Ni}_{80}\text{Fe}_{20}$ films doped with the lanthanides Gd, Tb, Dy, and Ho. By varying the dopant concentration we were able to tune the damping parameter by 2 orders of magnitude. The dynamic response was measured over a wide frequency range (0.5–35 GHz). By employing various resonance techniques and configurations extrinsic and intrinsic relaxation effects are separated. This procedure allows us to precisely determine the induced damping for the various rare earth dopants and, more importantly, to unambiguously identify the physical origin of the effect. We find that the slow relaxation of the $4f$ electron spins of the rare earth atoms is responsible for the induced damping. As this mechanism should also lead to a very strong temperature dependence of the relaxation, we perform temperature dependent ferromagnetic resonance (FMR) measurements to test the applicability of the slow relaxer model.

A series of 10 and 30 nm thick RE-doped $\text{Ni}_{80}\text{Fe}_{20}$ films was grown by dc magnetron cosputtering from single element targets. A 1 nm thick Ta seed layer was first deposited onto the glass substrates. The RE-doped $\text{Ni}_{80}\text{Fe}_{20}$ films were capped with a 3 nm thick Ta layer to prevent oxidation. During deposition an Ar gas pressure of

2×10^{-3} mbar was used and the deposition rate was about 0.1 nm/s. The film thicknesses of all samples were measured by x-ray reflectivity, and the RE concentration was determined by Rutherford backscattering; the uncertainty of this method is below 1 at. %. The static properties of the samples were investigated by vibrating sample magnetometry and magneto-optic Kerr effect measurements. In $\text{Ni}_{80}\text{Fe}_{20}$ -RE intermetallic alloys the $4f$ magnetic moments of the RE atoms are coupled to the $3d$ moments of the $\text{Ni}_{80}\text{Fe}_{20}$ via the intra-atomic $5d$ orbitals [4,5]. The resulting effective $4f$ - $3d$ exchange coupling is antiferromagnetic leading to an antiparallel alignment of RE $4f$ moments and the $\text{Ni}_{80}\text{Fe}_{20}$ $3d$ moments [4,5]. This ferromagnetic order leads to a decreasing saturation magnetization with increasing RE content. In our samples we observe a linear decrease of the saturation magnetization

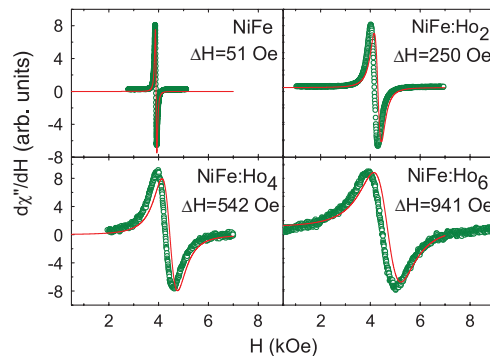


FIG. 1 (color). FMR spectra for four different Ho doping concentrations measured at room temperature (RT) in the in-plane configuration using a frequency of 22 GHz. The red lines show the expected FMR lines given by the saturation magnetization, the g factor, and the damping constant. In the calculation the upshift of the resonance field with increasing doping is caused by the decreasing magnetization. The g factor was determined by out-of-plane FMR measurements and remains nearly unchanged up to a doping level of 6%. Note that for the 6% sample the discrepancy between the expected and the measured line position is about 300 Oe.

as a function of doping for all RE elements with a slope of about 40 emu/cm^3 per atomic percent of RE doping at room temperature (RT). All samples have soft magnetic properties with small coercive fields (less than 2 Oe) and small uniaxial anisotropy fields (less than 5 Oe). From a structural point of view, all samples discussed in this Letter exhibit a polycrystalline fcc structure typical for the low RE concentrations (below 8%) used here [1]. However, clustering of the RE atoms does not occur even in the amorphous phase at much higher RE concentrations [6].

In ferromagnetic resonance measurements the linewidth $\Delta H(f)$ is proportional to the microwave frequency f only for Gilbert damping. Two magnon scattering due to defects and the superposition of local resonance lines due to large scale magnetic inhomogeneities lead to a zero frequency linewidth $\Delta H(0)$ [7,8]. If Gilbert damping dominates, one has $\Delta H(0) \ll \Delta H$ and the linewidth at a given frequency can be converted into the damping parameter using $\alpha = \Delta H \gamma / \omega$.

The series of FMR lines shown in Fig. 1 was measured at a frequency of 22 GHz using Ho concentrations of 0%–6%. These data illustrate the broadening of the FMR linewidth as a function of the rare earth concentration. The pure $\text{Ni}_{80}\text{Fe}_{20}$ film exhibits a linewidth of approximately 50 Oe whereas ΔH increases by a factor of 20 up to 940 Oe for a Ho concentration of 6%.

The observed linewidth broadening can generally have various origins. In order to be able to distinguish contributions from (i) Gilbert damping, (ii) two magnon scattering, and (iii) sample inhomogeneity, we perform FMR measurements over a wide frequency range allowing us to estimate $\Delta H(0)$ and thus to verify whether significant extrinsic contributions are present. Out-of-plane FMR measurements further allow one to separate magnetic inhomogeneity (local resonance) and two magnon scattering contributions [7,9] as for inhomogeneous samples one expects a line broadening in the perpendicular configuration compared to the parallel configuration ($\Delta H_{\perp} > \Delta H_{\parallel}$) [10]. For all samples discussed in this Letter the out-of-

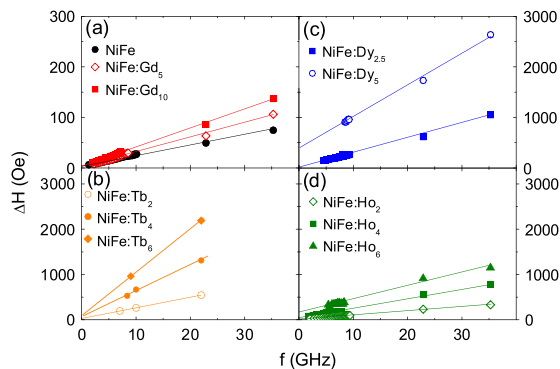


FIG. 2 (color online). Frequency dependence of ΔH for (a) $\text{Ni}_{80}\text{Fe}_{20}$ and Gd doped $\text{Ni}_{80}\text{Fe}_{20}$, (b) Tb doped $\text{Ni}_{80}\text{Fe}_{20}$, (c) Dy doped $\text{Ni}_{80}\text{Fe}_{20}$, and (d) Ho doped $\text{Ni}_{80}\text{Fe}_{20}$ films. All measurements are carried out in the parallel configuration at RT.

plane angular dependence of ΔH (not shown) is consistent with Gilbert damping and we observe $\Delta H_{\perp} \approx \Delta H_{\parallel}$.

Figure 2 shows the FMR linewidth as a function of frequency for various concentrations of Gd, Tb, Dy, and Ho. The linewidth strongly increases with increasing Tb, Dy, and Ho doping concentration, while almost no effect is observed for Gd doping (note the $10\times$ reduced scale for Gd doping). For all films at doping levels of 6% and below, the linewidth at zero frequency $\Delta H(0)$ is very small compared to the total linewidth at 22 GHz and can be neglected. We conclude that for doping concentrations up to 6% for all RE dopants the parameter α can be easily determined from the slope of the frequency dependent linewidth. The results are summarized in Fig. 3.

For Gd doping of 5% the damping constant of the $\text{Ni}_{80}\text{Fe}_{20}$ film is not considerably influenced. On the other hand, Ho, Tb, and Dy doped $\text{Ni}_{80}\text{Fe}_{20}$ films show a very strong dependence of the damping parameter on the dopant concentration. With increasing RE concentration the damping parameter α increases linearly. From the slope of the linear increase we determine the contribution to the damping parameter per concentration of RE dopant, i.e., $\alpha = \alpha_{\text{NiFe}} + \Delta\alpha_{\text{RE}} C_{\text{RE}}$, where C_{RE} is the RE atomic concentration in percent. The values for $\Delta\alpha_{\text{RE}}$ are 0.0005, 0.038, 0.036, and 0.017 for Gd, Tb, Dy, and Ho. We observe that $\Delta\alpha_{\text{RE}}$ for Tb and Dy doping are similar and lead to the largest damping, while the value for Ho is only about half that of Tb and Dy. For Gd doping the contribution is very small and only a consequence of the reduced magnetization.

This is a striking observation considering that earlier experimental [2] and theoretical [11] studies suggested RE-induced damping to be proportional to the orbital moment of the dopants. Based on these predictions one should observe the largest effect for Ho ($L = 6$), a smaller effect for Dy ($L = 5$) and Tb ($L = 3$), and no effect for Gd ($L = 0$). This behavior is not observed in our detailed measurements. In Fig. 4 the contributed damping parameter $\Delta\alpha_{\text{RE}}$ is plotted as a function of the orbital moment of the dopants. Clearly the contributed damping is not proportional to the orbital moment of the dopants.

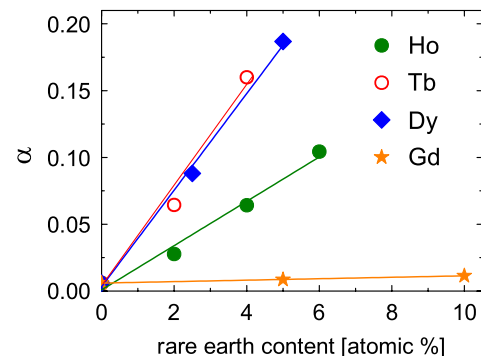


FIG. 3 (color online). Damping parameter α determined from the slope of $\Delta H(f)$ shown in Fig. 2 as a function of the RE concentration.

In the 1960s van Vleck and Orbach [12] introduced the “slow relaxing” impurity model to describe the damping in RE-doped yttrium iron garnets (YIG) [13]. The essence of the slow relaxer model is the following: the $4f$ multiplet of the RE is split in the moderate exchange field of the $5d$ electrons. This Zeeman splitting is of the order of 10 meV and the levels are hence thermally populated at RT. The anisotropy of the $4f$ - $5d$ exchange interaction causes a modulation of the $4f$ exchange splitting when the $3d$ moments precess. The thermal population of the $4f$ levels follows this temporal modulation, but it is delayed by the RE relaxation time τ_{RE} . Thermal transitions in the $4f$ multiplet lead to a locally fluctuating transverse field $h(t)$ acting on the $3d$ moments via the strong $3d$ - $5d$ coupling if the $4f$ - $5d$ exchange interaction is anisotropic. Using the second fluctuation dissipation theorem one can show that the damping constant is given by the Fourier transform of the time correlation of $h(t)$ [14]. The time correlation function of the fluctuation field can be approximated by $\langle h(t)h(0) \rangle = h^2 \exp(-t/\tau)$ leading to the following expression for the Gilbert damping parameter:

$$\alpha_{\text{RE}} = CF(T) \left[\frac{\tau_{\text{RE}}}{1 + (\omega\tau_{\text{RE}})^2} + i \frac{\omega\tau_{\text{RE}}^2}{1 + (\omega\tau_{\text{RE}})^2} \right], \quad (1)$$

where the constant C is given by $C = \frac{AC_{\text{RE}}}{6M_S k_B T}$ and the temperature dependent function $F(T)$ accounts for the fact that the precession induced repopulation of the $4f$ levels strongly depends on the temperature [15]. M_S is the saturation magnetization, C_{RE} is the concentration of the RE ions, and A is the anisotropy of the $5d$ - $4f$ exchange interaction and given by the angular derivatives of the $5d$ - $4f$ exchange energy $\hbar\Omega$ [15]. Its magnitude can be estimated from the anisotropy contribution arising from

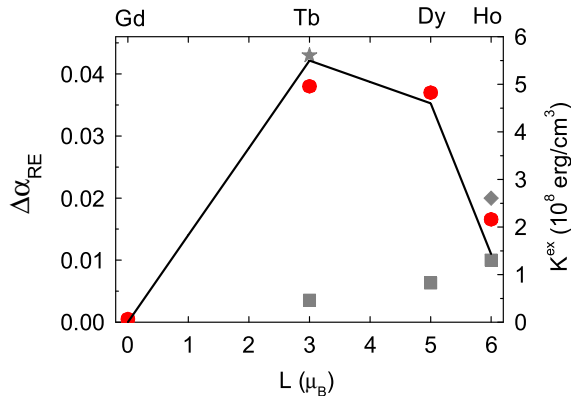


FIG. 4 (color online). Comparison of the contributed damping $\Delta\alpha_{\text{RE}}$ (red bullets) to the anisotropy contribution arising from the anisotropic exchange interaction between the $4f$ moments and the conduction electrons K^{ex} (black line) as a function of orbital moment L [16]. In addition, values of RE-induced damping in $\text{Ni}_{80}\text{Fe}_{20}$ are plotted from Refs. [2] (gray squares), [1,19] (gray star), and [20] (gray diamond). In Ref. [2] the damping is given as relaxation rates λ . These numbers were converted into Gilbert damping using $\alpha = \lambda/(\gamma 4\pi M)$.

the anisotropic exchange interaction between the $4f$ moments and the conduction electrons as observed in metallic rare earth single crystals K^{ex} [16]. For a two level system one has $F(T) = \text{sech}^2 \frac{\hbar\Omega}{k_B T}$ [15]. The population of the $4f$ levels in RE-doped YIG is indeed well described as a two level system due to the large crystal field splitting. In experiments both ΔH_{RE} and S_{RE} have shown a strong temperature dependence with a peak occurring at low T when $\hbar\Omega = k_B T$ [13,15,17]. The two level approximation, however, may not be justified for RE-doped $\text{Ni}_{80}\text{Fe}_{20}$. Because of the absence of a significant crystal field in the metallic alloy $2J + 1$ $4f$ levels need to be considered allowing transitions to occur at possibly $2J$ different energies. Therefore considerable broadening of the linewidth peak at low temperature (compared to RE-doped YIG) is expected for RE-doped $\text{Ni}_{80}\text{Fe}_{20}$.

The real part of Eq. (1) corresponds to damping and causes a linewidth $\Delta H_{\text{RE}} = \text{Re}(\alpha) \frac{\omega}{\gamma}$ while the imaginary part leads to a negative field shift $S_{\text{RE}} = -\text{Im}(\alpha) \frac{\omega}{\gamma}$. Provided that $\omega \ll 1/\tau_{\text{RE}}$ the damping is independent of the frequency and the resonance field shift is small. The negative field shift is a consequence of the time delayed damping torque (due to thermal repopulation of the $4f$ levels) leading to an effective longitudinal field.

In order to predict the relative strength of this effect at a given temperature as a function of the RE element, one only needs to compare the calculated relative magnitude of the anisotropic exchange contribution to the magnetic anisotropy [16] as shown in Fig. 4. One finds $K_{\text{Gd}}^{\text{ex}} = 0$, $K_{\text{Tb}}^{\text{ex}} = 5.5 \times 10^8 \text{ erg/cm}^3$, $K_{\text{Dy}}^{\text{ex}} = 4.6 \times 10^8 \text{ erg/cm}^3$,

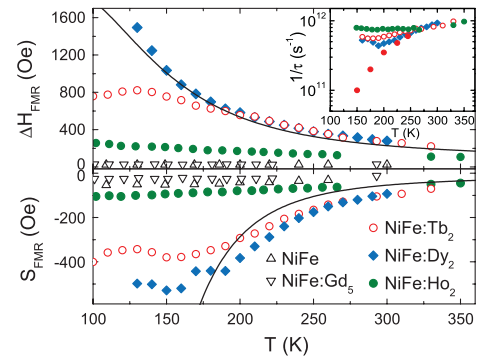


FIG. 5 (color). Temperature dependence of the FMR linewidth (ΔH) and the FMR field shift S for a dopant concentration of 2.0% for Tb and Ho, 2.5% for Dy, and 5% for Gd. The measurements were carried out at 10 GHz in the parallel configuration. The field shift S corresponds to the difference between the resonance fields of the doped and undoped samples. Note that the data for 2.5% Dy were multiplied by $4/5$ in order to be able to compare them to the Tb and Ho 2.0% data. The solid lines represent the expected behavior and were calculated from Eq. (1) by using three $4f$ transition energies. For the temperature dependence τ_{RE} we used Eq. (13) of [17]. The inset shows the temperature dependence of τ_{RE} as determined from the present FMR measurements. The red bullets represent earlier measurement of τ_{RE} for Nd doped YIG [17].

and $K_{\text{Ho}}^{\text{ex}} = 1.43 \times 10^8 \text{ erg/cm}^3$ [16]. Neglecting the temperature dependence in Eq. (1) (it should be roughly the same for the various RE elements), one immediately observes that the RE-induced relaxation should be significantly smaller for Ho dopants compared to Tb and Dy. It is also apparent from this analysis why doping with Gd with its isotropic $4f$ - $5d$ exchange interaction (S state) cannot lead to additional relaxation.

The applicability of the slow relaxing model for RE-doped $\text{Ni}_{80}\text{Fe}_{20}$ can be further tested by verifying whether ΔH_{RE} and S_{RE} increase with decreasing temperature as predicted by Eq. (1). Figure 5 shows the temperature dependence of ΔH_{RE} and S_{RE} measured at $f = 10 \text{ GHz}$ for $\text{Ni}_{80}\text{Fe}_{20}$, $\text{Ni}_{80}\text{Fe}_{20}:\text{Gd}_5$, $\text{Ni}_{80}\text{Fe}_{20}:\text{Tb}_2$, $\text{Ni}_{80}\text{Fe}_{20}:\text{Dy}_{2.5}$, and $\text{Ni}_{80}\text{Fe}_{20}:\text{Ho}_2$. Indeed for Tb, Dy, and Ho, the data can be well described by Eq. (1). The expected negative field shift of the resonance field is clearly observed; see Fig. 5. The temperature dependence of ΔH_{RE} and S_{RE} is expected to be similar since it is primarily caused by $F(T)$ and $\tau_{\text{RE}}(T)$. Using Eq. (1) the RE relaxation time τ_{RE} can be estimated from the ratio $2|S_{\text{RE}}|/\Delta H_{\text{RE}} = \omega\tau_{\text{RE}}$. From the data shown in Fig. 5 for S_{RE} and ΔH_{RE} , one can estimate at room temperature $\tau_{\text{RE}}^{300\text{K}} \sim 1 \text{ ps}$ and at low temperature $\tau_{\text{RE}}^{120\text{K}} \sim 3\text{--}10 \text{ ps}$ for Tb, Dy, and Ho doping. This is in excellent agreement with earlier independent measurements [17] for τ_{RE} observed in RE-doped YIG as can be seen in the inset of Fig. 5. The shorter $\tau_{\text{RE}}^{300\text{K}}$ causes the field shift to be rather small at RT; cf. Fig. 1. As $\omega\tau_{\text{RE}} \ll 1$ for all our measurements, Eq. (1) predicts a linear frequency dependence of the FMR linewidth in agreement with the experimental results shown in Fig. 2.

In addition to the temperature dependence, the magnitude of the RE-induced linewidth is similar for YIG and $\text{Ni}_{80}\text{Fe}_{20}$ if one considers the ratio of RE concentration to the magnetization. By scaling the YIG results from Dillon [18] one expects for a doping level of 2% at room temperature a linewidth of a few hundred Oe at 10 GHz for RE = Tb and Dy—in agreement with the present results; see Fig. 5. It is therefore compelling to conclude that the additional damping due to RE doping in $\text{Ni}_{80}\text{Fe}_{20}$ is caused by the very same slow relaxing impurity mechanism which was originally proposed for RE-doped YIG.

Our experimental results sharply contradict earlier experimental [2] and theoretical work [11]. Reidy *et al.* [2] performed dynamic measurements using pulsed inductive magnetometry at very low frequencies ($\sim 500 \text{ MHz}$). In addition, these measurements suffer from a large uncertainty with respect to the RE content of the samples. The corresponding data points are included in Fig. 4. The absolute values for the damping constants derived from those measurements are up to a factor of 5 lower than our present results. However, we would like to point out that our present results are in excellent agreement with earlier measurements for Tb doped $\text{Ni}_{80}\text{Fe}_{20}$ films deposited under similar conditions as the films used in the present study [1,19] (see Fig. 4). Bailey *et al.* found a strong

dependence of the contributed damping on the Ar pressure during the film deposition [1], with larger damping observed in films deposited at lower sputter gas pressures. Lower sputter gas pressures and lower deposition rates typically lead to smoother, more homogeneous films with larger grain sizes. Note that the films used in the present study were deposited at even lower sputter gas pressures and deposition rates than the ones in [1]. The theoretical work by Rebei and Hohlfield [11] is based on orbit-orbit coupling effects between RE impurities and itinerant electrons but does not consider the slow relaxing impurity model. Rebei *et al.* solely justify the itinerant treatment of $4f$ electrons on the basis of better agreement with the experimental data by Reidy *et al.* [2]. However, their theory results in temperature independent Gilbert damping without a negative field shift and strictly proportional to the orbital moment of the RE impurities. These predictions are clearly at variance with our experimental results. On the other hand, the present results (temperature, frequency, and element dependence of the RE-induced damping) can be readily explained by the slow relaxing impurity model.

This work was supported in part by the German Research Foundation through programs SFB 689 and SPP 1133. Professor B. Heinrich and Professor C.E. Patton are acknowledged for helpful comments. G.M. acknowledges support from the AvH foundation.

-
- [1] W.E. Bailey, P. Kabos, F. Mancoff, and S. Russek, *IEEE Trans. Magn.* **37**, 1749 (2001).
 - [2] S.G. Reidy, L. Cheng, and W.E. Bailey, *Appl. Phys. Lett.* **82**, 1254 (2003).
 - [3] J.O. Rantschler *et al.*, *J. Appl. Phys.* **101**, 033911 (2007).
 - [4] I.A. Campbell, *J. Phys. F* **2**, L47 (1972).
 - [5] H.S. Li and J.M.D. Coey, *J. Phys. Condens. Matter* **3**, 7277 (1991).
 - [6] C.J. Robinson *et al.*, *Appl. Phys. A* **49**, 619 (1989).
 - [7] R.D. McMichael, D.J. Twisselmann, and A. Kunz, *Phys. Rev. Lett.* **90**, 227601 (2003).
 - [8] B. Heinrich, F. Cochran, and R. Hasegawa, *J. Appl. Phys.* **57**, 3590 (1985).
 - [9] R. Arias and D.L. Mills, *Phys. Rev. B* **60**, 7395 (1999).
 - [10] J.A. Bland and B. Heinrich, *Ultrathin Magnetic Structures III* (Springer-Verlag, Berlin, 2005).
 - [11] A. Rebei and J. Hohlfield, *Phys. Rev. Lett.* **97**, 117601 (2006).
 - [12] J.H. van Vleck and R. Orbach, *Phys. Rev. Lett.* **11**, 65 (1963).
 - [13] P.E. Seiden, *Phys. Rev.* **133**, A728 (1964).
 - [14] B. Heinrich and A.S. Arrott, *AIP Conf. Proc.* **34**, 119 (1976).
 - [15] M. Sparks, *J. Appl. Phys.* **38**, 1031 (1967).
 - [16] Yu.P. Irkin, *Sov. Phys. JETP* **154**, 321 (1988).
 - [17] B.H. Clarke, *Phys. Rev.* **139**, A1944 (1965).
 - [18] J.F. Dillon, *Phys. Rev.* **127**, 1495 (1962).
 - [19] S.E. Russek *et al.*, *J. Appl. Phys.* **91**, 8659 (2002).
 - [20] N. Benatmane, T.F. Ambrose, and T.W. Clinton, *J. Appl. Phys.* **105**, 07D314 (2009).